

# Fertilization

## Michelle Plachot

Laboratoire de FIV, Hôpital de Sèvres, 141, Grande Rue, 92311 Sèvres, France

*Assistant Professor INSERM and Director of the IVF Laboratory, Sèvres Hospital, France. Current research interests are embryo development and preimplantation genetics*

Fertilization is a process that culminates in the union of the maternal and paternal pronuclei, leading to the formation of a new individual (for reviews, see Crozet, 1993; Van Blerkom *et al.*, 1995; Brewis and Moore, 1997; Benoff, 1997).

For this process to occur successfully, several events must take place: (i) sperm penetration of the cumulus oophorus; (ii) sperm interaction with the zona pellucida; (iii) sperm–oocyte fusion; (iv) oocyte activation; (v) decondensation of the sperm nucleus and pronucleus (PN) formation; (vi) development of the male and female pronuclei and their migration to the centre of the oocyte; and (vii) association of the parental chromosomes on the spindle of the first cleavage division.

In humans, as in most mammalian species, the ovulated oocyte, which is arrested in metaphase of the second meiotic division (MII), is surrounded by an expanded cumulus composed of follicular cells dispersed in a polymerized matrix composed mainly of hyaluronic acid. Spermatozoa penetrating the cumulus are generally capacitated. In contrast to other species, sperm capacitation in humans requires a very short time, as IVF has been achieved after only 45 min of contact between oocytes and spermatozoa capacitated for 1 h (Figure 3.1; Plachot *et al.*, 1986). Before penetrating the zona pellucida, spermatozoa must bind to it and undergo the acrosome reaction. The oocyte-specific zona pellucida glycoprotein 3 (ZP3) serves as both the primary ligand for sperm binding and as a trigger for the acrosome reaction in the fertilizing spermatozoa.

The acrosome reaction is an exocytotic event involving multiple fusions between the sperm plasma membrane and the outer acrosomal membrane, resulting in the formation of hybrid membrane vesicles. It leads to the  $\text{Ca}^{2+}$ -dependent externalization of the contents of the acrosomal vesicles. After zona penetration, the sperm head crosses the perivitelline space and fuses with the oocyte membrane in a highly specific manner, inducing oocyte activation. In humans, although several spermatozoa bind to the zona pellucida, only one usually reaches the perivitelline space. Fertilization failure may be due to non-accomplishment of sperm–zona binding or to incomplete zona penetration (2/3 through the zona). The mechanism of oocyte activation has not been completely elucidated, but changes in membrane potential and a dramatic

increase in intracellular  $\text{Ca}^{2+}$  are known to be early events in this phenomenon. Morphological changes that take place in the activated oocyte, e.g. cortical granule exocytosis, completion of the second meiotic division and modification of the oocyte cortex are well documented.

Exocytosis of cortical granules occurs in response to intracellular  $\text{Ca}^{2+}$  mobilization (Figure 3.2). Cortical granules contain hydrolytic enzymes that are released into the perivitelline space by exocytosis. These enzymes modify the chemical and physical characteristics of the zona pellucida, rendering it impenetrable to spermatozoa. The failure of cortical granule exocytosis permits polyspermy. Upon activation by the spermatozoon, the oocyte resumes meiosis, proceeding to anaphase and then to telophase and finally dividing into two unequal cells: the fertilized oocyte and the second polar body, each of which contain half of the maternal DNA. The consequence of this asymmetric division is that most of the molecules and information stored during oogenesis that are necessary for early development are retained in the oocyte cytoplasm (Figures 3.3 and 3.4).

After incorporation into the oocyte cytoplasm, the sperm nucleus undergoes a series of transformations, e.g. nuclear envelope disintegration, reduction of the disulphide bonds of DNA-associated protamines, chromatin decondensation and replacement of sperm-specific protamines by histones. At the same time, maternal chromatin progresses from metaphase to interphase. The pronuclei are then formed by the development of nuclear envelopes around the male and female chromatin and rapid decondensation of parental chromatin. Active DNA synthesis takes place simultaneously in both well-developed pronuclei (Figures 3.5–3.11). Apposition of the pronuclei in the centre of the oocyte is a prerequisite for paternal and maternal chromosome assembly on the spindle of the first cleavage division. The sperm centrosome duplicates and separates to become the future poles of the first mitotic spindle (Sathananthan *et al.*, 1996). Failure of the sperm aster microtubules to unite the sperm and oocyte nuclei may be a cause of fertilization failure (Navara *et al.*, 1997).

## The first cell cycle of human zygotes

The diagram illustrates the approximate timing of events taking place during the first cell cycle of human zygotes. The lines represent subsequent phases of the cycle and indicate the time range between the appearance of the first and last zygotes in a particular phase. The duration of the full cell cycle seems to be ~20–22 h, but considerable asynchrony is observed among the zygotes (Figures 3.12 and 3.13). Variations in cycle dynamics may be due to the time of oocyte fertilization (IVF/ICSI), the intrinsic properties of the gametes and in-vitro culture condi-

**Table I.** Approximate timing of events occurring in the first cell cycle of human zygotes (conventional IVF)

Phase	Approximate length of each phase (h)	Time of zygote appearance (hpi)	
		First	Last
Extrusion of second polar body	2–3	2–3	10
G <sub>1</sub> phase	5–6	2–3	14
S phase	4–5	8–14	20–24
G <sub>2</sub> phase	5–6	12–14	28–30
M-phase	3–4	17–22	30–31
2-cell stage		20–25	33–34

hpi = hours post-insemination.

tions. Therefore, the full length of each phase may differ among zygotes derived from a single cohort of oocytes. For instance, second polar body (2PB) extrusion in ICSI oocytes may occur 1–8 h after injection. Oocytes fertilized by ICSI usually undergo pronucleus development and the first cleavage division ~2–4 h earlier than oocytes derived from standard IVF. Such differences probably relate to the difference in the time of sperm penetration. The cell cycle of polyspermic zygotes (3PN) seems to be similar to that of normal zygotes (2PN) except that in some cases cleavage is delayed due to chromosomal/spindle abnormality. However, despite the cycle variations, the following general conclusions can be drawn: (i) The G<sub>1</sub> phase begins with the formation of the 2PB and completion of the second meiotic division. Many zygotes enter G<sub>1</sub> phase by 3 h post-insemination (especially ICSI zygotes) and by 14 h post-insemination the majority of zygotes have completed this phase; (ii) DNA synthesis begins between 8 and 14 h post-insemination and is completed between 14 and 24 h post-insemination; (iii) the first zygotes in G<sub>2</sub> phase appear at ~12 h post-insemination and the last at ~30–31 h post-insemination; and (iv) the duration of M-phase is relatively constant (median 3 h, range 3–4 h). Chromosome condensation begins at 17–18 h post-insemination. The majority of zygotes undergo pronuclear breakdown and the first division between 24 and 30 h post-insemination and 27 and 33 h post-insemination respectively (for reviews, see Balakier *et al.*, 1993; Nagy *et al.*, 1995; Drozortsev *et al.*, 1995; Campany *et al.*, 1996; Payne *et al.*, 1997).

### Fertilization abnormalities

Premature sperm chromosome condensation (PCC) and formation of one or three pronuclei are the most frequently observed fertilization abnormalities (Plachot and Crozet, 1992). PCC is characterized by the presence of sperm chromatids in inseminated mature or immature oocytes that have failed to form pronuclei and are therefore considered to be unfertilized (Figure 3.14). PCC occurs in ~10–50% of supposedly unfertilized oocytes and seems to be the consequence of a failure of oocyte activation, leading to the maintenance of cytoplasmic chromosome-condensing factors, causing the sperm nucleus to undergo chromosome condensation prematurely. This anomaly appears to be related to incomplete nuclear and/or cytoplasmic maturation.

Although not an abnormality of fertilization, the formation of oocytes with only one pronucleus results from failure of the fertilization process (Figure 3.15). It occurs in ~1% of oocytes after IVF or ICSI. Cytogenetic analysis shows that in ~50% of cases the oocyte has a haploid chromosome constitution, suggesting a parthenogenetic origin. Oocytes with a single pronucleus may also result from asynchrony in pronucleus development (with a second pronucleus appearing a few hours later) or in rare cases from pronucleus fusion. In this case, a diploid zygote is formed.

Tripronuclear zygotes may result from digyny or diandry (Figure 3.16). The extra chromosome set of digynic triploids is of maternal origin and may result from fertilization of a diploid oocyte (with the non-reduced number of chromosomes) by a normal (haploid) spermatozoon. Conversely, the extra chromosome set in diandric triploids is of paternal origin and may result from dispermic fertilization. Most of the triploid zygotes observed following IVF result from diandry, whereas all of those observed following ICSI result from digyny because a single spermatozoon is injected. Triploid zygotes form in ~5% of inseminated oocytes (after IVF) and 1% of microinjected oocytes (after ICSI). DNA synthesis in triploid zygotes is represented in Figures 3.17–3.21. After IVF, some 3PN zygotes divide into three cells via a tripolar spindle (Figure 3.22; Plachot and Crozet, 1992; Balakier, 1993). This accounts for the chaotic chromosome constitution generally observed in embryos developing from 3PN zygotes resulting from IVF. Other fertilization abnormalities are shown in Figures 3.23–3.28.

### Failed cleavage

Some oocytes arrest at the pronuclear stage. This could be due either to failed ooplasmic activation (Tesarik and Sousa, 1995) or to defects associated with the spermatozoon. Among them, incomplete sperm nucleus migration, incorrect centrosomal location, and dispersed chromatin distribution may be possible causes (Van Blerkom *et al.*, 1995; Sathananthan *et al.*, 1996).

### References

- Balakier, H. (1993) Tripronuclear human zygotes: the first cell cycle and subsequent development. *Hum. Reprod.*, **8**, 1892–1897.
- Balakier, H., MacLusky, N.J. and Casper, R.F. (1993) Characterisation of the first cell cycle in human zygotes: implication for cryopreservation. *Fertil. Steril.*, **59**, 359–365.
- Benoff, S. (1997) Carbohydrates and fertilization: an overview. *Mol. Hum. Reprod.*, **3**, 599–637.
- Brewis, I.A. and Moore, D.M. (1997) Molecular mechanisms of gamete recognition and fusion at fertilization. *Hum. Reprod.*, **12** (Nat. Suppl.), JBFS, **2**, 156–165.
- Campany, G., Taylor, A., Braude, P.R. *et al.* (1996) The timing of pronuclear formation, DNA synthesis and cleavage in the human 1-cell embryo. *Mol. Hum. Reprod.*, **2**, 299–306.
- Crozet, N. (1993) Fertilisation *in vivo* and *in vitro*. In Thibault, C., Levasseur, M.C. and Hunter, R.H.F. (eds), *Reproduction in Mammals and Man*. Ellipses, Paris, France, pp. 327–347.
- Drozortsev, D., De Sutter, P., Rybouchkin, A. *et al.* (1995) Timing of sperm and oocyte nuclear progression after intracytoplasmic sperm injection. *Hum. Reprod.*, **10**, 3012–3017.
- Hartshorne, G.M., Blayney, M., Dyson, H. and Elder, K. (1990) Case Report: In vitro fertilization and development of one of two human oocytes with fused zona pellucida. *Fertil. Steril.*, **54**, 947–949.

- Hartshorne, G. (1989) A simple method for the morphological analysis of human ova: zona penetration in oocytes failing to fertilize or fertilizing abnormally *in vitro*. *Hum. Reprod.*, **4**, 588–594.
- Nagy, Z.P., Liu, J., Joris, H. *et al.* (1995) Time-course of oocyte activation, pronuclear formation and cleavage in human oocytes fertilized by intracytoplasmic sperm injection. *Hum. Reprod.*, **9**, 1743–1748.
- Navara, C.S., Hewitson, L.C., Simerly, C.R. *et al.* (1997) The implications of a paternally derived centrosome during human fertilisation: consequences for reproduction and the treatment of male factor infertility. *Am. J. Reprod. Immunol.*, **37**, 39–49.
- Payne, D., Flaherty, S.P., Barry, M.F. *et al.* (1997) Preliminary observations on polar body extrusion and pronuclear formation in human oocytes using time-lapse video cinematography. *Hum. Reprod.*, **12**, 532–541.
- Plachot, M., Junca, A.M., Mandelbaum, J. *et al.* (1986) Timing of in-vitro fertilization of cumulus-free and cumulus-enclosed human oocytes. *Hum. Reprod.*, **1**, 237–242.
- Plachot, M. and Crozet, N. (1992) Fertilization abnormalities in human in-vitro fertilization. *Hum. Reprod.*, **7** (Suppl. 1), 89–94.
- Sathanathan, A.H., Ratnam, S.S., Ng, S.C. *et al.* (1996) The sperm centriole: its inheritance, replication and perpetuation in early human embryos. *Hum. Reprod.*, **11**, 345–356.
- Tesarik, J. and Sousa, M. (1995) More than 90% fertilisation rate after intracytoplasmic sperm injection and artificial induction of oocyte activation with calcium ionophore. *Fertil. Steril.*, **63**, 343–349.
- Van Blerkom, J., Davis, P., Merriam, J. *et al.* (1995) Nuclear and cytoplasmic dynamics of sperm penetration, pronuclear formation and microtubule organization during fertilization and early preimplantation development in the human. *Hum. Reprod. Update*, **1**, 429–461.
- Van Steirteghem, A.C., Joris, H., Liu, J. *et al.* (1995) Protocol for intracytoplasmic sperm injection. *Hum. Reprod. Update*, **1**(3) CD Rom Item 9.

## Figure Legends

### Figure 3.1

Sections (5  $\mu\text{m}$ ) through inseminated oocytes. (3.1.1) Spermatozoa in the perivitelline space, 30 min post-insemination. (3.1.2) Spermatozoon entering the oocyte 45 min post-insemination (courtesy of M.Plachot, Paris, France).

### Figure 3.2

Resin section (1  $\mu\text{m}$ ) through unfertilized oocyte, stained with Toluidine Blue. Note cortical granules at periphery of oocyte, stained blue. Two spermatozoa are trapped in the zona pellucida (courtesy of G.Hartshorne, Warwick, UK. Published with permission from Hartshorne, G.M., *Hum. Reprod.* (1989) 4, 588–594).

### Figure 3.3

Zygote with two polar bodies far apart in the perivitelline space (courtesy of A.De Vos, Brussels, Belgium. Published with permission from Van Steirteghem, A.C., Joris, H., Liu, J. *et al.* *Hum. Reprod. Update* (1995) CD Rom Item 9).

### Figure 3.4

Large sized second polar body with a nucleus evident, at 16 h after ICSI (magnification  $\times 200$ ). Analogous to the observations in mice, a large sized first or second polar body is often termed immediate cleavage (courtesy of L.Gianaroli, Bologna, Italy).

### Figures 3.5–3.11

Different phases of DNA synthesis in two pronuclear human zygotes derived from conventional IVF procedure. Replication of DNA was determined by examining radioactive [ $^3\text{H}$ ]-thymidine incorporation by the pronuclei at various times during the first cell cycle of the zygotes. The pictures show the pronuclei on serial sections (1–5  $\mu\text{m}$ ; zygotes fixed with 2.5% glutaraldehyde and 2% osmium tetroxide; embedded in plastic) (courtesy of H.Balakier, Toronto, Canada. Published with permission from Balakier, H., MacLusky, N.J. and Casper, R.F. *Fertil. Steril.* (1993) 59, 359–365).

### Figure 3.5

Two pronuclei exhibiting intense DNA synthesis are uniformly saturated with radioactive thymidine grains. Fixed at 11 h post-insemination; original magnification  $\times 3200$ .

### Figures 3.6 and 3.7

Two pronuclei showing moderate DNA synthesis. Radioactive grains are accumulated along the nuclear membranes and nucleoli. The interior of the pronuclei remains unlabelled. Fixed at 11 h post-insemination; original magnification  $\times 3200$ .

### Figure 3.8

Weak asynchronous DNA synthesis in two pronuclei. One pronucleus shows some radioactive label whereas the other has only few grains. The uneven distribution of the grains within the nuclei was apparent in the series of sections, indicating asynchronous DNA synthesis. The second polar body contains heavy thymidine incorporation indicating intense DNA synthesis. Fixed at 13 h post-insemination; original magnification  $\times 2600$ .

### Figure 3.9

Large adhering pronuclei in  $G_2$  phase of the first cycle. Radioactive label in pronuclei is not detectable. Fixed at 22 h post-insemination; original magnification  $\times 2600$ .

### Figures 3.10 and 3.11

Two pronuclei from the same human zygote fixed by the air-drying technique. The whole pronuclear spreads exhibit heavy thymidine incorporation over the nuclear threads indicating intense DNA

synthesis. Fixed at 13 h post-insemination; original magnification  $\times 2100$ .

### Figure 3.12

Diagrammatic representation of the first cell cycle of human zygotes; hpi = hours post insemination.

### Figure 3.13

Extrusion of the second polar body (1 h 50 min to 2 h after ICSI). The first polar body is clearly evident at the 12 o'clock position. The second polar body starts to appear at the 11:30 position (3.13.1,3.13.2) and is completely extruded in (3.13.3). Appearance of pronuclei at (3.13.4) 6 (3.13.5) 6.5 (3.13.6) 7 (3.13.7) 8 (3.13.8) 8.5 (3.13.9) 9 and (3.13.10) 9.5 h after ICSI. The axis of the two pronuclei forms a right angle to the longitudinal axis passing through the small area between the polar bodies. The nucleoli are located in a specific orientation (original magnification  $\times 200$ ) (courtesy of L.Gianaroli, Bologna, Italy).

### Figure 3.14

Prematurely condensed chromosomes ( $G_1$ -PCC) of the sperm nucleus (2c) after ICSI. The maternal MII chromosomes and the polar body chromatin (pb) (1b) of the oocyte (inset in a; magnification  $\times 400$ ) are also visible. The regions numbered 1 and 2 in the overall view are shown at higher magnification ( $\times 2000$ ). The inset oocyte is at a magnification of  $\times 187.5$  (courtesy of H.Schmiady, Berlin, Germany).

### Figure 3.15

One pronuclear oocyte with two polar bodies. Both polar bodies are split (courtesy of A.De Vos, Brussels, Belgium. Permission as in 3.3).

### Figure 3.16

Tripronuclear oocyte with one polar body (courtesy of A.De Vos, Brussels, Belgium. Permission as in 3.3).

### Figure 3.17

Three pronuclei undergoing intense DNA synthesis indicated by heavy thymidine incorporation. Fixed at 11 hpi, original magnification  $\times 3000$  (courtesy of H.Balakier, Toronto, Canada. Published with permission from Balakier, H. *Hum. Reprod.* (1993) 8, 1892–1897).

### Figure 3.18

Three pronuclei exhibiting moderate DNA synthesis. Thymidine incorporation is present only along the nuclear membranes and nucleoli. Fixed at 13 hpi; original magnification  $\times 3000$  (courtesy of H.Balakier, Toronto, Canada. Permission as in 3.17).

### Figure 3.19

Triploid zygote in the course of  $G_2$  phase of the first cell cycle. Pronuclear radioactive labelling is not visible. The second polar body contains several grains indicating DNA replication. Fixed at 22 hpi; original magnification  $\times 2600$  (courtesy of H.Balakier, Toronto, Canada. Permission as in 3.17).

### Figures 3.20 and 3.21

Three whole pronuclear spreads saturated with radioactive thymidine that indicates heavy DNA replication. One pronucleus (3.20) was apart from the others (3.21) and was photographed separately. Fixed at 11 hpi; original magnification  $\times 2800$  (courtesy of H.Balakier, Toronto, Canada. Permission as in 3.17).

**Figure 3.22**

Tripronuclear zygote showing a tripolar spindle. (3.22.1) Tripolar spindle assessed by anti-tubulin antibodies. (3.22.2) Chromosomes with a Y configuration stained with Hoechst dye (courtesy of M.Plachot, Paris, France).

**Figure 3.23**

Oocyte with four pronuclei at 16 h post-insemination (magnification  $\times 400$ ) (courtesy of M.C.Magli, Bologna, Italy).

**Figure 3.24**

Paired oocytes joined at the zona pellucida. The cumulus was removed with hyaluronidase. (3.24.1) Two pronuclei are visible in the large oocyte and a germinal vesicle in the smaller (20 h post-insemination). (3.24.2) Blastocyst and adjoined egg on day 7 post-insemination (courtesy of G.Hartshorne, Warwick, UK. Reprinted with permission from American Society of Reproductive Medicine, *Fertil. Steril.*, 54, 947–949).

**Figure 3.25**

In spite of this oocyte unhealthy appearance with zona pellucida and cytoplasmic irregularities, (3.25.1) two pronuclei were

observed 18 h post-insemination and (3.25.2) two regular blastomeres 48 h post-insemination (original magnification  $\times 400$ ) (courtesy of S.Nikolaropoulos, Athens, Greece).

**Figure 3.26**

(3.26.1) Abnormal oocyte with oval shape and a large perivitelline space at fertilization control; (3.26.2) total fragmentation observed 24 h later (courtesy of M.Plachot, Paris, France).

**Figure 3.27**

Elongated zona, irregularly shaped zygote with a large perivitelline space (original magnification  $\times 200$ ) (courtesy of L.Gianaroli, Bologna, Italy).

**Figure 3.28**

Abnormal oocyte (16 h after ICSI): oval shape, augmented perivitelline space, remnants of the first polar body, irregular cytokinesis with extrusion of a large second polar body (original magnification  $\times 200$ ). This is another example of immediate cleavage, with two unequally sized pronuclei evident in the smaller half (courtesy of L.Gianaroli, Bologna, Italy).

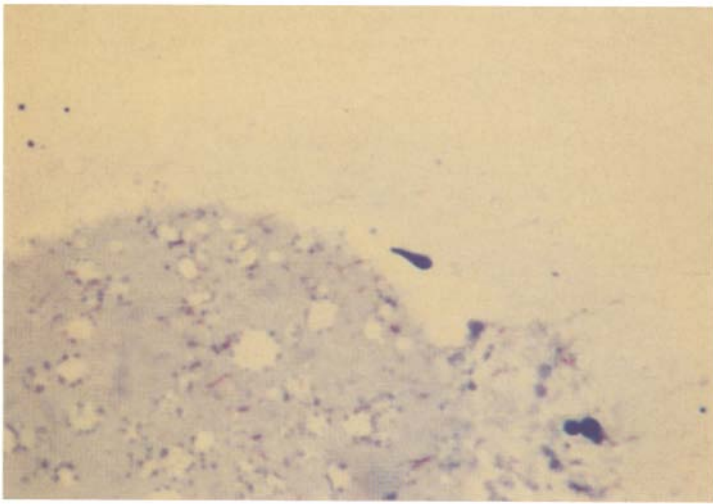


Figure 3.1.1

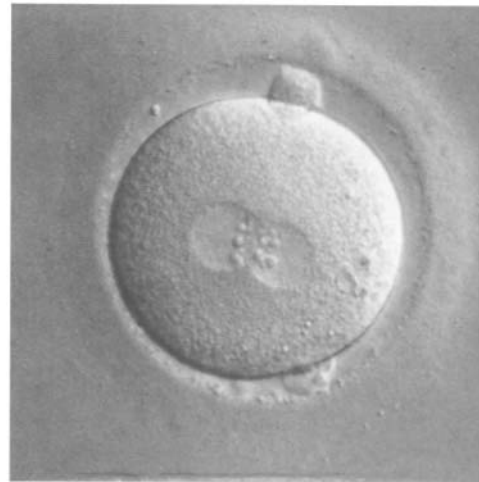


Figure 3.3

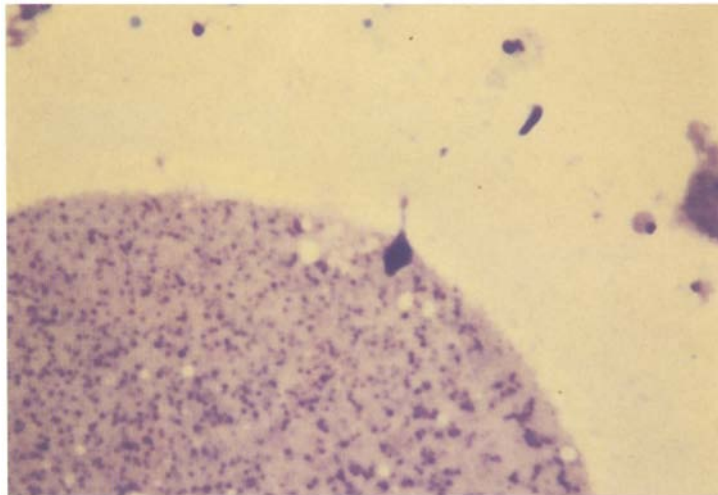


Figure 3.1.2

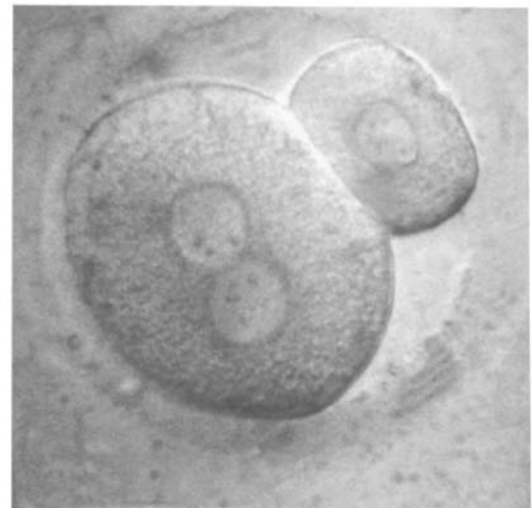


Figure 3.4

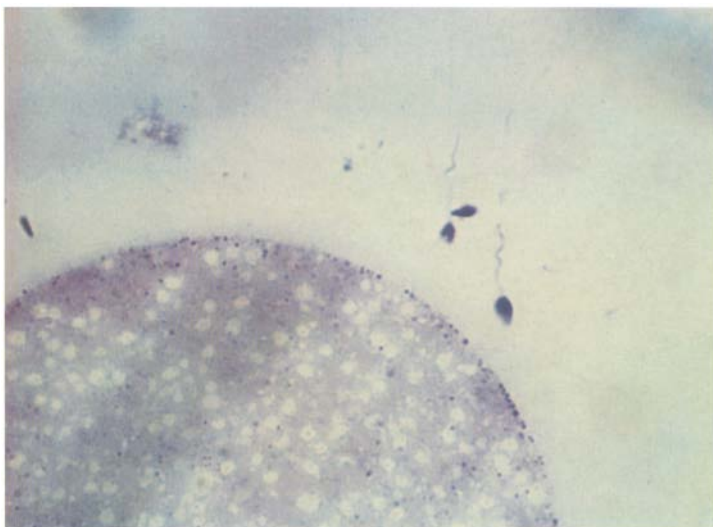


Figure 3.2

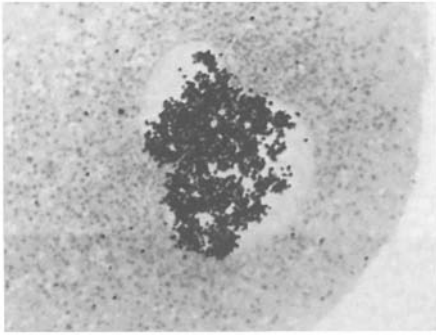


Figure 3.5

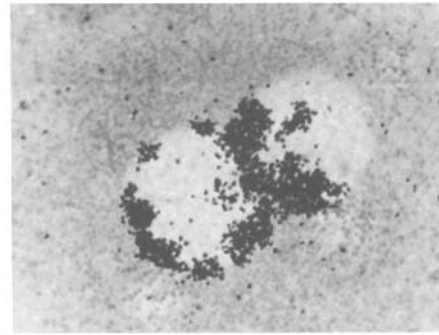


Figure 3.6

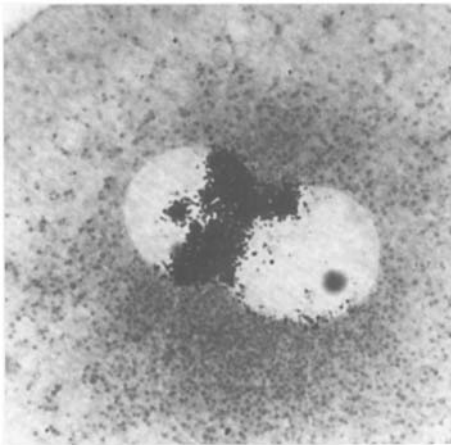


Figure 3.7

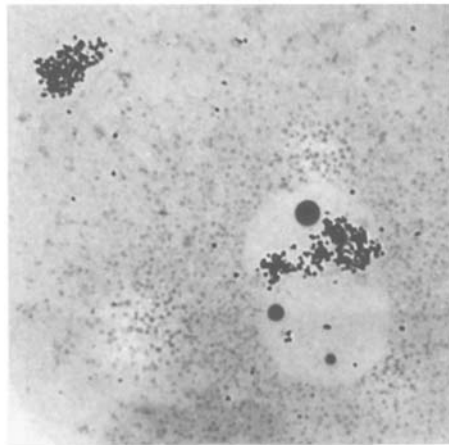


Figure 3.8

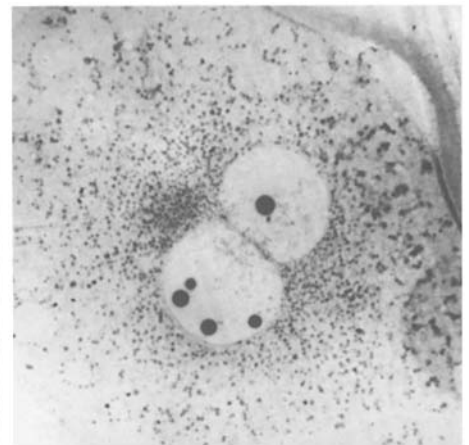


Figure 3.9



Figure 3.10

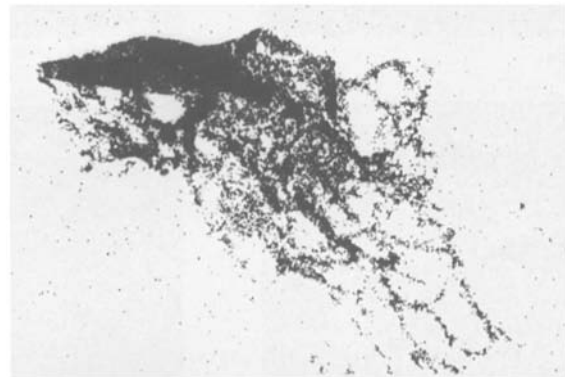


Figure 3.11

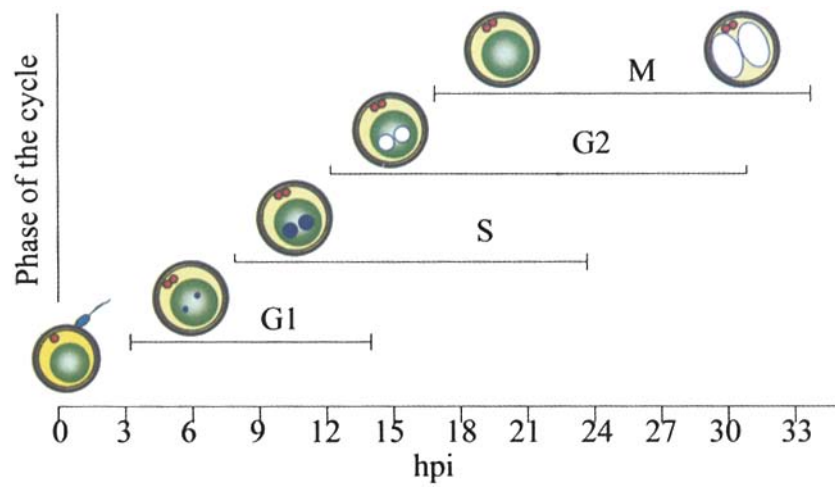


Figure 3.12

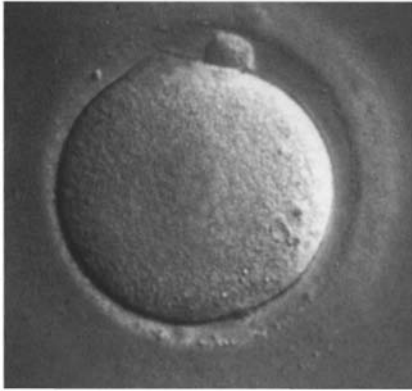


Figure 3.13.1

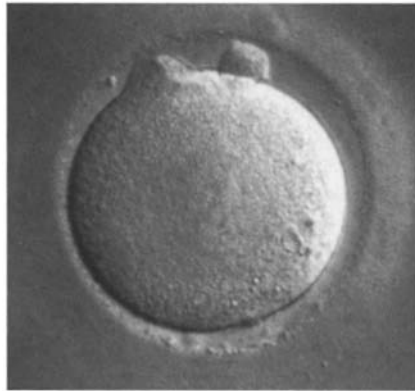


Figure 3.13.2

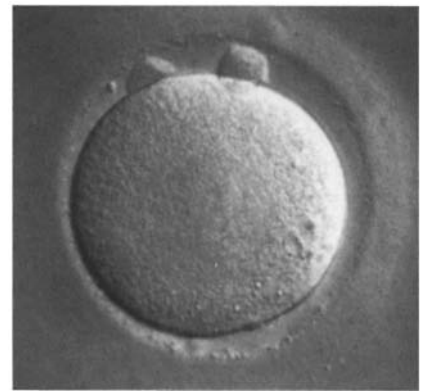


Figure 3.13.3

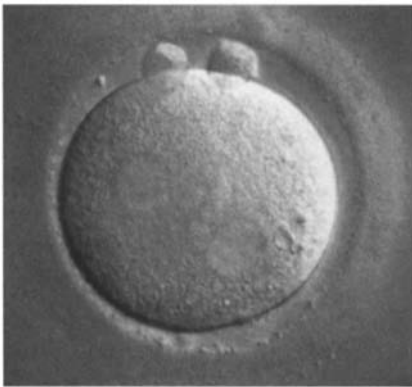


Figure 3.13.4

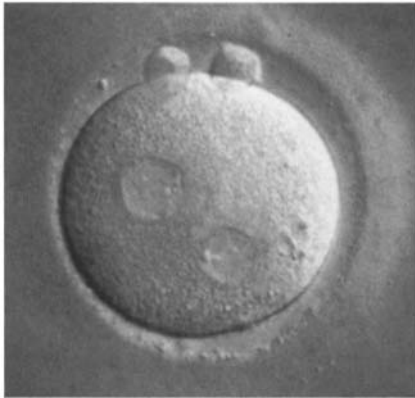


Figure 3.13.5

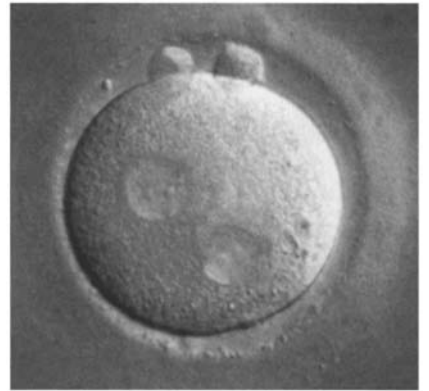


Figure 3.13.6

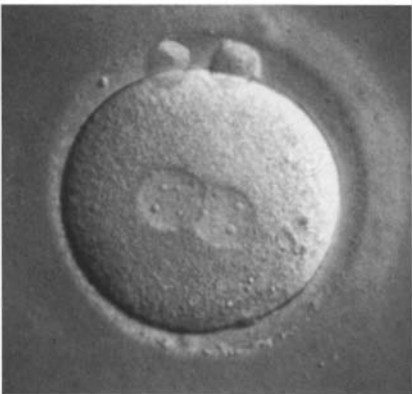


Figure 3.13.7

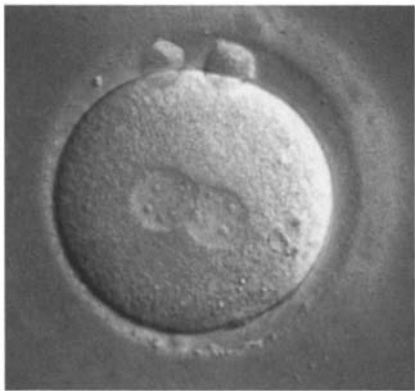


Figure 3.13.8

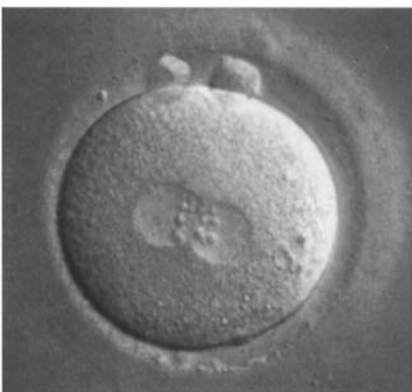


Figure 3.13.9

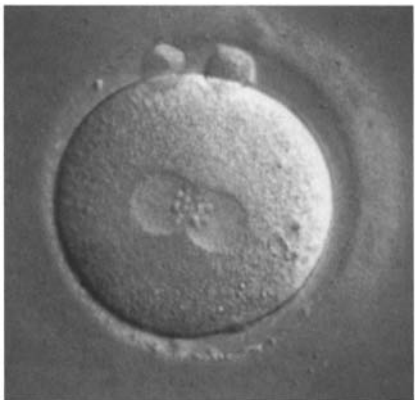


Figure 3.13.10

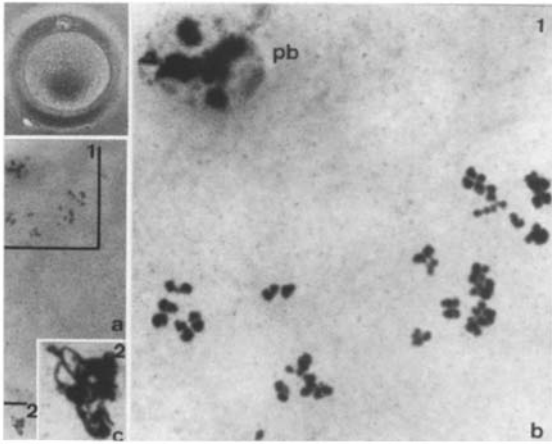


Figure 3.14

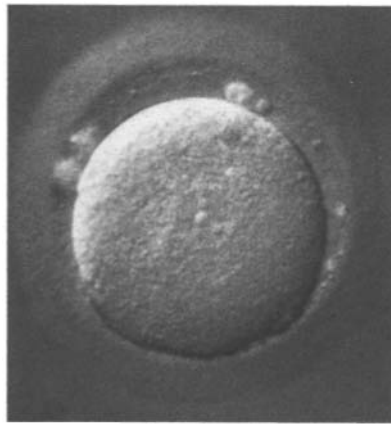


Figure 3.15



Figure 3.16

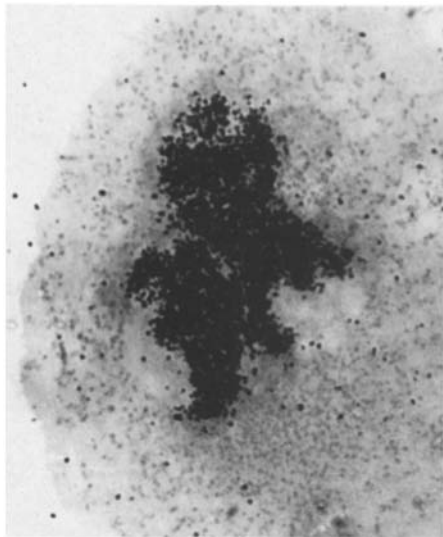


Figure 3.17

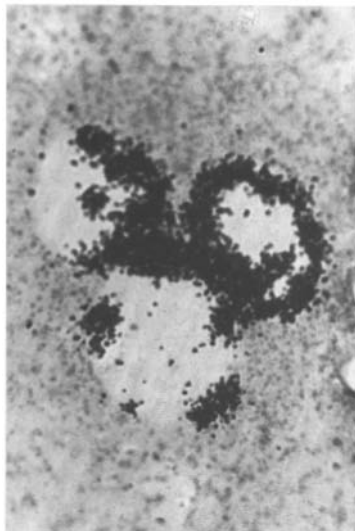


Figure 3.18

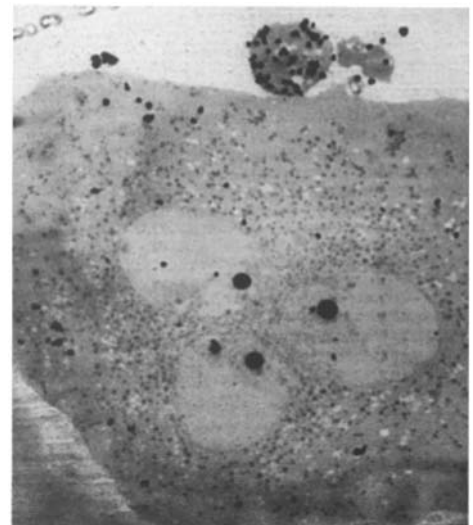


Figure 3.19

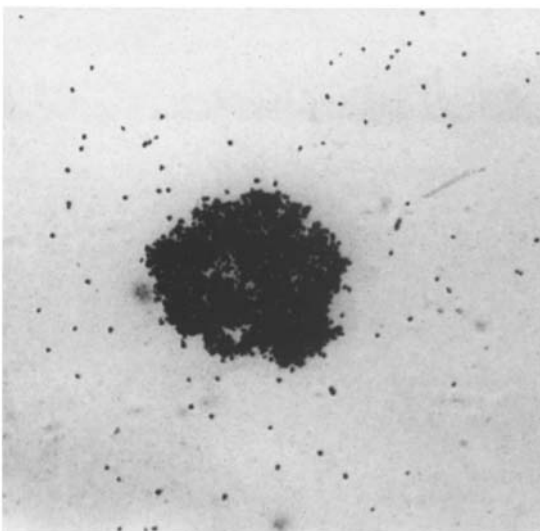


Figure 3.20

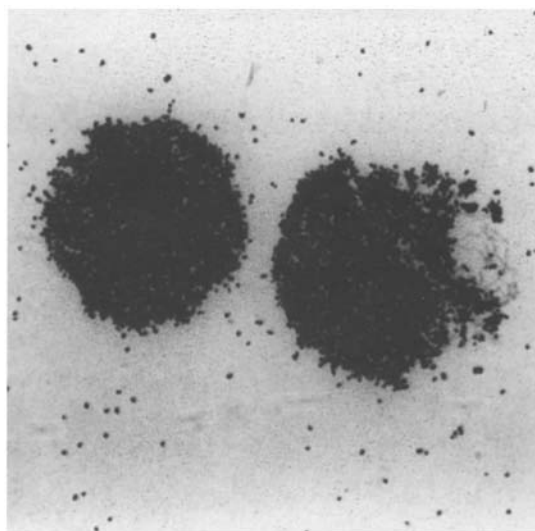


Figure 3.21

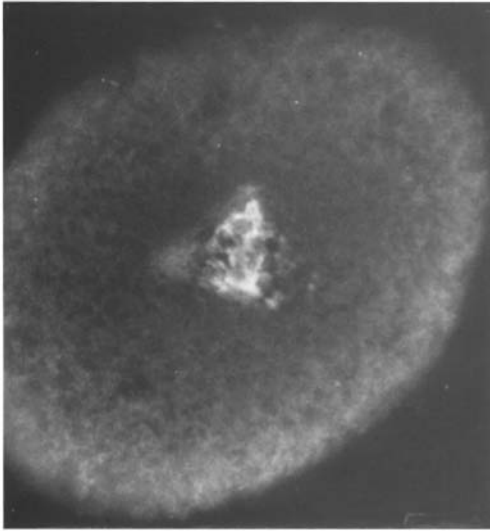


Figure 3.22.1



Figure 3.22.2

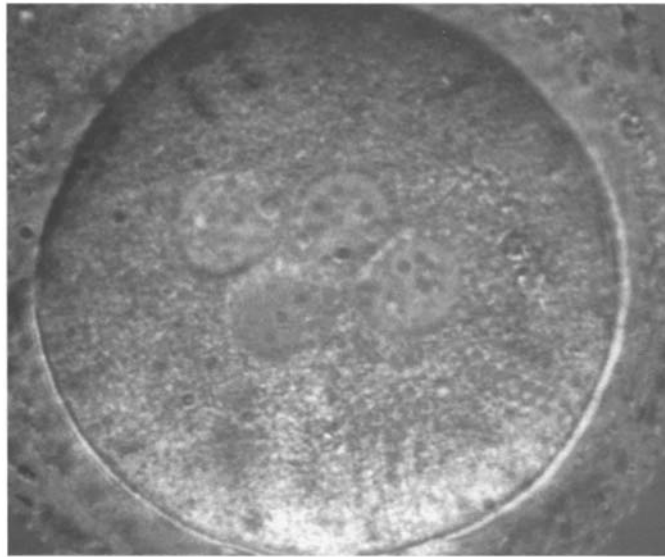


Figure 3.23

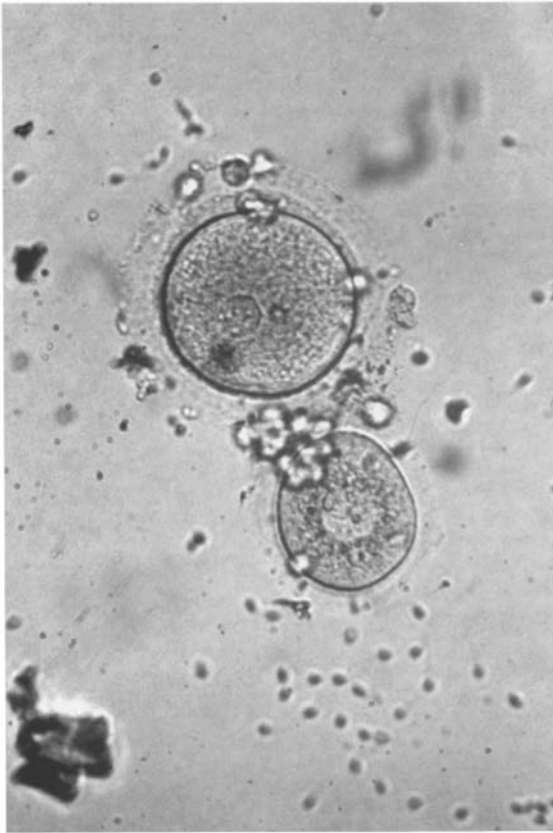


Figure 3.24.1



Figure 3.24.2

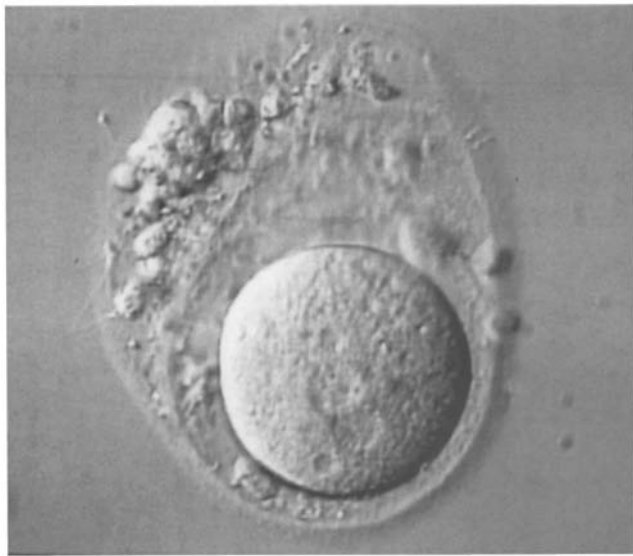


Figure 3.25.1



Figure 3.25.2

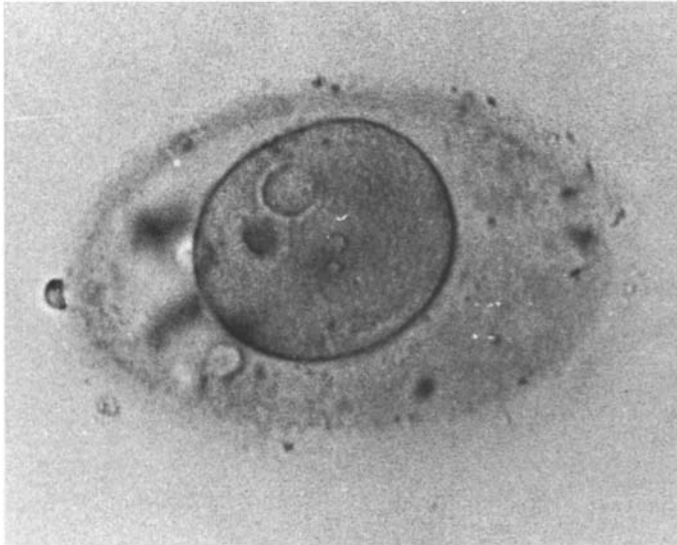


Figure 3.26.1



Figure 3.26.2

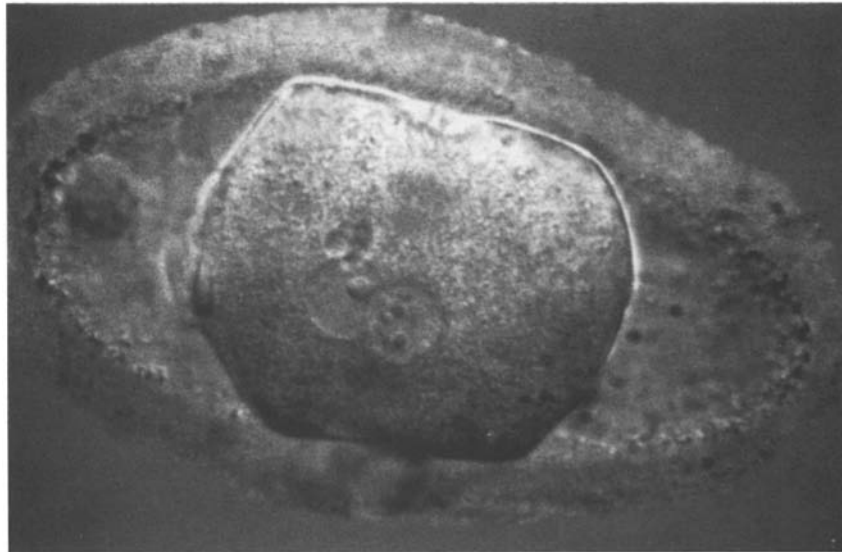


Figure 3.27



Figure 3.28